Mitochondrial reactive oxygen species mediate metabolic stability

by

Samantha Steyl

Honors Thesis

Appalachian State University

Submitted to the Department of Chemistry
and The Honors College
in partial fulfillment of the requirements for the degree of

Bachelor of Science

May, 2018

Approved by:

_____
Brooke Christian, Ph.D., Thesis Director

_____
Darren Seals, Ph.D., Second Reader

_____
Megen Culpepper, Ph.D., Third Reader

_____
Libby Puckett, Ph.D., Departmental Honors Director

_____
Jefford Vahlbusch, Ph.D., Dean, The Honors College

Abstract

Oxidative phosphorylation (OXPHOS) is the metabolic pathway in mitochondria that produces the large majority of ATP used by the cell. Superoxide, a reactive oxygen species (ROS), is generated during OXPHOS when electrons are prematurely transferred to oxygen. Although ROS are necessary for certain cell signaling pathways, they are generally thought to be damaging to the cell. Cells can protect themselves against oxidative damage using antioxidant enzymes that break down superoxide and other ROS. Antioxidants are currently used as therapeutics for a number of diseases, but so far, mitochondria targeted antioxidants have not been well characterized for this purpose. Manganese superoxide dismutase (SOD2) is an antioxidant enzyme found in mitochondria that converts superoxide into hydrogen peroxide. This project focuses on mice that overexpress SOD2. Microarray analysis of gene expression in these mice showed potentially defective OXPHOS gene expression. Preliminary studies confirmed reductions of complexes II and III in the SOD2 samples by sodium dodecyl sulfate polyacrylamide gel electrophoresis (SDS-PAGE), and a reduction of complex II assembly in the SOD2 liver samples by blue native PAGE. Current studies have shown that SOD2 mice have reduced assembly of complex II and V by BN-PAGE, but unchanged assembly of complexes I and III by the same method. To follow up on these results, activity assays indicate a decrease in complex II activity and a potential increase in complex I activity. Aconitase showed an increase in activity in SOD2 samples as well. Taken together, this implicates that overexpression of SOD2 causes defects in OXPHOS.

Introduction

Relevance

Free radicals are generated in mitochondria as a byproduct of oxidative phosphorylation and can be damaging to the cell. Oxidative damage can have major health consequences, and can contribute to various diseases such as cancer, aging, diabetes, and Alzheimer's disease.[3-6] The health benefits of antioxidants, which eliminate reactive oxygen species, are well recognized but are mechanistically not well understood. This project focuses on investigating the physiological consequences of targeted antioxidants. A preliminary microarray was conducted using RNA isolated from livers of mice that overexpress the mitochondrial antioxidant enzyme superoxide dismutase. Although it was expected that increased detoxification of superoxide would be beneficial to oxidative phosphorylation, gene expression analysis actually showed potential defects. Since reactive oxygen species are known to participate as signaling molecules in a number of pathways, it is possible that high levels of antioxidants could be detrimental. This study has important implications for antioxidant therapeutics, specifically when used to treat diseases characterized by impaired liver function.

Mitochondria and Oxidative Phosphorylation

Mitochondria are dual-membrane organelles found in eukaryotes that are responsible for oxygen consumption and ATP production.[7] Oxidative phosphorylation (OXPHOS) is the metabolic pathway in mitochondria that generates a large majority of cellular ATP. During OXPHOS, a series of oxidation-reduction reactions transfer electrons from NADH and $FADH_2$ through four electron transport complexes and ultimately to

molecular oxygen to form water.[8] These four multi-subunit complexes are NADH dehydrogenase (complex I; 45 proteins), succinate dehydrogenase (complex II; 4 proteins), ubiquinone-cytochrome c oxidoreductase (complex III; 11 proteins), and cytochrome c oxidase (complex IV; 13 proteins). As electrons flow, complexes I, III, and IV pump protons across the inner mitochondrial membrane into the intermembrane space (Figure 1). The proton gradient generated in the intermembrane space provides chemiosmotic energy to drive ATP production as protons move back across the membrane through ATP synthase (complex V; 17 proteins). All OXPHOS complexes, with the exception of complex II, contain critical proteins that are encoded in mitochondrial DNA.

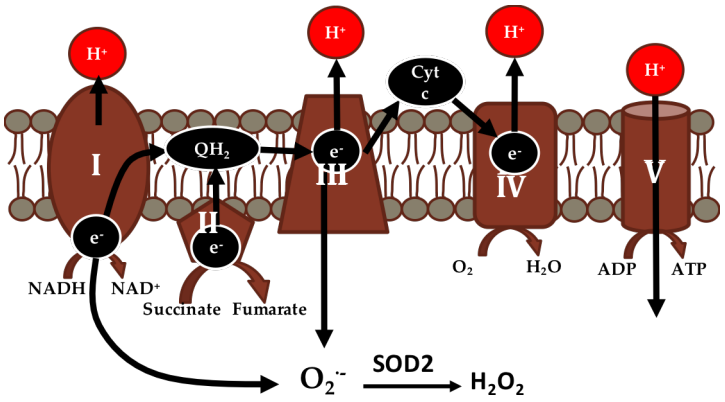

Figure 1. Oxidative phosphorylation in mitochondria. The transfer of electrons from NADH and $FADH_2$ through complexes I through IV reduces oxygen to form water. Alternatively, electrons can be prematurely transferred to oxygen to form the superoxide radical, $O_2^{\cdot-}$. Proton-coupled electron transfer generates a proton gradient that drives ATP synthesis. Figure modified from Ethan Sarnoski, unpublished.

Mitochondrial DNA

Mitochondria are specialized organelles that have their own genome. Mitochondrial DNA (mtDNA) is maternally inherited and is a closed circular DNA molecule composed of ~17,000 base pairs (Figure 2).[9] Each eukaryotic cell contains 100-10,000 copies of mtDNA.[10] mtDNA encodes two ribosomal RNAs, 22 transfer RNAs, and

13 proteins.[9] All 13 proteins encoded in mtDNA are essential components of OXPHOS complexes. mtDNA is replicated, transcribed, and translated within the organelle, and all enzymes responsible for these processes are encoded in nuclear DNA.[11] Mitochondria and prokaryotes have many similarities, and it is thought that mitochondria evolved from an endosymbiotic relationship between a bacterial cell and its host.[11]

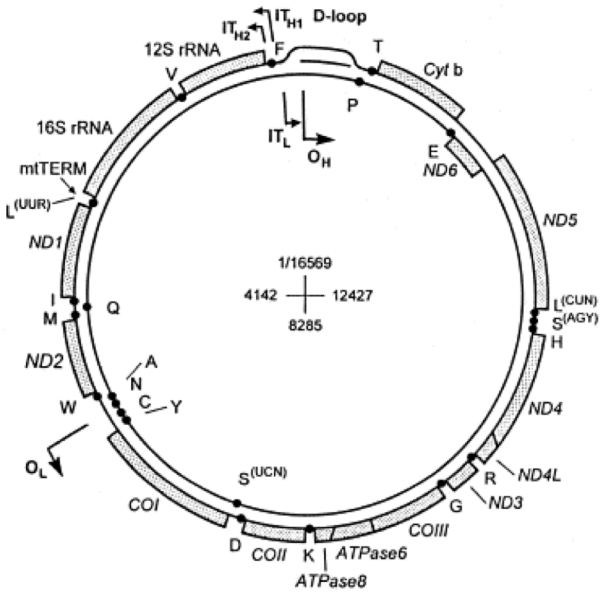

Figure 2. The mitochondrial genome. mtDNA encodes 13 proteins involved in OXPHOS. NADH dehydrogenase (ND), ubiquinone cytochrome c oxidoreductase (Cyt b), cytochrome c oxidase (CO), and ATP synthase (ATPase) contain subunits encoded within the mitochondrial genome. Figure reproduced with permission.[1]

OXPHOS requires 90 proteins, 13 of which are encoded in mtDNA (Figure 2) and 77 of which are encoded in nuclear DNA. Complex I contains 7 mitochondrial subunits (*ND1, ND2, ND3, ND4L, ND4, ND5* and *ND6*) and 38 nuclear subunits. In complex III, 1 of the 11 proteins (*Cyt b)* is encoded by mtDNA. Complex IV contains 3 mitochondria-encoded subunits (*CO*I, *COII*, and *COIII*) of 13 total, and ATP synthase has 2 of its 17 proteins (*ATPase6* and *ATPase8*) encoded in mtDNA. Proteins that compose complex II are all encoded by nuclear DNA. Since functional oxidative phosphorylation requires assembly of protein subunits from both the nuclear and mitochondrial genomes, close coordination of gene expression must be maintained between the mitochondria and the nucleus.

Reactive Oxygen Species and Antioxidants

During OXPHOS, electrons can be prematurely transferred to oxygen to generate reactive oxygen species (ROS), specifically superoxide. Superoxide is a radical that contains a single unpaired electron and is converted in mitochondria to hydrogen peroxide (H_2O_2) by manganese superoxide dismutase (SOD2). Hydrogen peroxide is membrane permeable and can leave the mitochondria, be reduced to water by catalase, or be reduced to the reactive hydroxyl radical (OH•) by the Fenton reaction with iron or copper.[12] Although small amounts of ROS are beneficial and can function as signaling molecules that contribute to pathways such as growth, metabolism, differentiation, and apoptosis, they are generally thought to be damaging at high concentrations.[12] Oxidative damage occurs when the amount of ROS generated exceeds antioxidant capacity.[13] At high levels, ROS can damage DNA, RNA, proteins, and lipids.[14] ROS can induce oxidation of guanine, resulting in the aberrant ability to base pair with adenine. ROS can oxidize and inactivate proteins and can cause lipid peroxidation. ROS damage to mitochondrial DNA can impair OXPHOS, leading to more ROS production and a vicious cycle that provides the basis for the free radical theory of aging.[15] ROS also contribute to various degenerative diseases and cancers.[16] Cells protect themselves against free radicals using antioxidant enzymes such as thioredoxin, glutathione peroxidase, peroxiredoxin, superoxide dismutases , and catalase.[17]

As previously mentioned, SOD2 is the focus of this project. SOD2 is an antioxidant enzyme that functions as a tetramer in the mitochondrial matrix and catalyzes the reaction of superoxide into hydrogen peroxide and oxygen using manganese as a cofactor (equation 1). [18]

$2O_2^{\bullet-} + 2H^+ \rightarrow H_2O_2 + O_2$ (Equation 1)

SOD2 reduces Mn^{3+} to Mn^{2+} and oxidizes superoxide to oxygen, then oxidizes Mn^{2+} back to Mn^{3+} to reduce superoxide to hydrogen peroxide. In this way, one molecule of superoxide is reduced and the other is oxidized.[18]

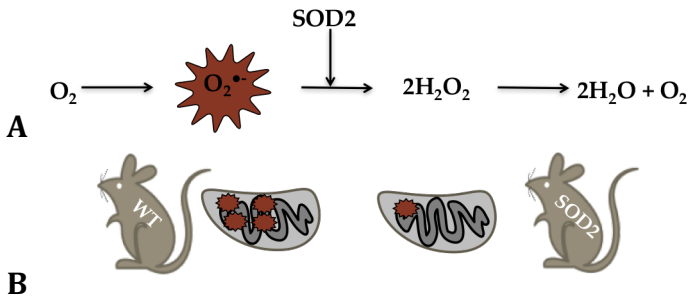

Figure 4. Experimental mouse model system. Mice overexpressing SOD2 have reduced superoxide levels. (**A**) SOD2 reduces superoxide to hydrogen peroxide which can be broken down into water and oxygen. (**B**) Mice with more SOD2 have less superoxide.

Mice that overexpress SOD2 have been developed and characterized[20] and are used in this project to identify genes responsive to mitochondrial ROS. These mice have reduced superoxide in mitochondria in various tissues including the liver, but the levels of hydrogen peroxide in these mice have not been determined (Figure 4). Although SOD2 is not the only enzyme that detoxifies superoxide, it is the only one that does so in the mitochondrial matrix, where the majority of cellular superoxide is produced. Copper/zinc SOD (SOD1) is a homodimer found in the cytosol, and also exists as a tetramer in the extracellular space (SOD3).[19, 21] In the electron transport chain, complexes I, II, and III contribute the most to the production of superoxide.[21]

Electron Transport Chain and OXPHOS

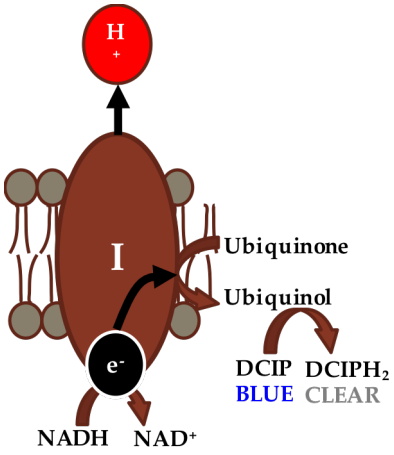

Figure 5. NADH dehydrogenase (complex I). Transfer of electrons occurs from NADH through complex I to ubiquinone, then to DCIP to form $DCIPH_2$.

NADH dehydrogenase (complex I) is the first of the four complexes in the electron transport chain (Figure 1). It is found in the mitochondrial inner membrane, and is responsible for oxidizing nicotinamide adenine dinucleotide hydride (NADH) to NAD^+ and transferring two electrons to ubiquinone (Figure 5).[22] Ubiquinone is a membrane-bound 2-electron carrier in the inner-mitochondrial membrane. Ubiquinone, when reduced to ubiquinol by complex I or II, can transfer electrons to complex III. If ubiquinone only accepts one electron, it becomes a radical and contributes to ROS production. This explains why complex I is a major source of ROS in the cell. In addition to transferring electrons, complex I pumps protons into the intermembrane space, contributing to the proton gradient used for ATP production. Specifically, four protons are pumped out of the mitochondrial matrix for every two electrons that are transferred through complex I.[22] To test for activity of complex I, NADH will be used as a substrate, and two electrons will be transferred through complex I to ubiquinone, then ultimately to the artificial electron acceptor DCIP. Reduction of DCIP causes a color change from blue to clear that can be measured in a spectrophotometer at 600 nm. Rotenone, an inhibitor of complex I, inhibits the transfer of electrons from complex I to ubiquinone.

Succinate dehydrogenase (complex II) is the second complex in the electron transport chain and is responsible for oxidizing succinate to fumarate. The oxidation of succinate is coupled with the reduction of a prosthetic group flavin adenine dinucleotide (FAD) to the dihydrate form $FADH_2$.[23] Electrons within complex II are ultimately transferred to ubiquinone (Figure 6). Ubiquinol is again used to carry electrons to complex III.[23] Complex II does not contribute to the proton gradient. However, with the transfer of electrons to FAD, complex II also contributes to the generation of ROS. Activity of complex II will be measured with succinate as a substrate and DCIP as the terminal electron acceptor.

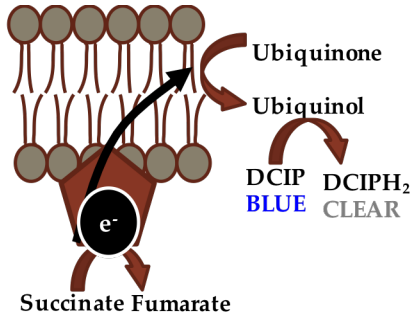

Figure 6. Succinate dehydrogenase (complex II). Electrons are transferred from succinate through complex II to reduce ubiquinone to ubiquinol.

Ubiquinone-cytochrome c oxidoreductase (Complex III) is the third complex in the electron transport chain, and is responsible for reducing two molecules of cytochrome c. Cytochrome c is a one-electron carrier that is not membrane bound.[24] The reduction of cytochrome c is coupled to oxidation of ubiquinol generated by complexes I and II (Figure 7). Since cytochrome c is a one-electron carrier, electrons from ubiquinol must be transferred one at a time. The transfer of a single electron generates a ubiquinone radical, which is

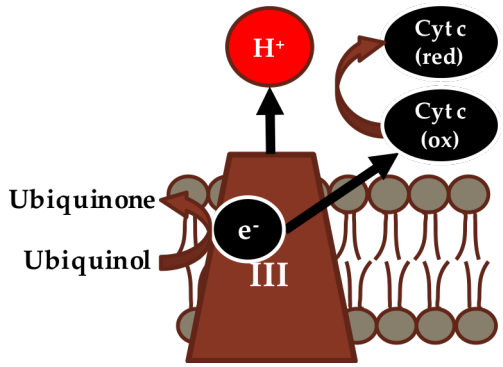

Figure 7. Ubiquinone-cytochrome c oxidoreductase (complex III). Electrons enter complex III as ubiquinol and are used to reduce cytochrome c. Transfer of electrons from ubiquinol to cytochrome c through complex III.

subsequently reduced during a second cycle of single electron transfer. However, the ubiquinone radical can donate its single electron to oxygen to produce a superoxide radical, which explains how complex III contributes to the generation of ROS.[25] Therefore, both ubiquinol molecules from complexes I and II enter complex III, and two cytochrome c molecules are reduced.[25] Four hydrogens are again pumped out of the mitochondrial matrix from Complex III into the intermembrane space to contribute to the proton gradient. antimycin A, an inhibitor of complex III, prevents ubiquinone from binding to cytochrome b.[26]

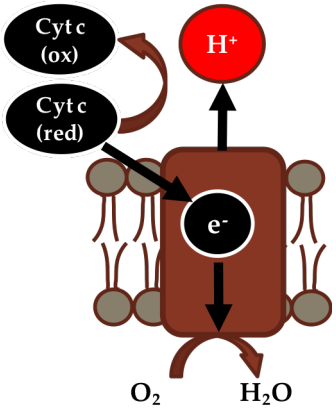

Figure 8. Cytochrome c oxidase (complex IV). Electrons from cytochrome c are transferred to oxygen to make water.

Cytochrome c oxidase (Complex IV) is responsible for oxidizing cytochrome c and reducing molecular oxygen to water (Figure 8). It is the last complex in the electron transport chain. Four reduced cytochrome c molecules are necessary to reduce one molecule of molecular oxygen to water.[27] Complex IV contributes four protons to the proton gradient.

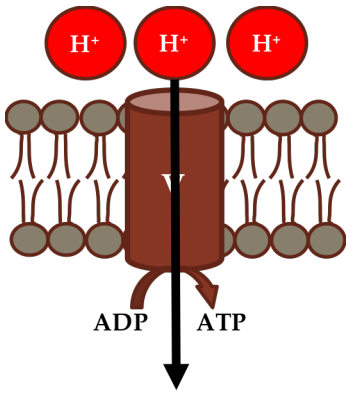

Figure 9. ATP synthase (complex V). The proton gradient generated in the intermembrane space provides energy to form energy from ADP and P_i.

ATP synthase (Complex V) is the final complex in oxidative phosphorylation and is responsible for the generation of ATP. The build-up of protons in the intermembrane space provides energy in the form of the proton gradient. As protons flow back into the matrix through complex V, energy from the proton motive force drives synthesis of ATP.[28] The formation of ATP occurs

in the matrix of the mitochondria (Figure 9). Adenosine diphosphate (ADP) and inorganic phosphate (P_i) are both necessary cofactors for the production of ATP.

The voltage dependent anion channel (VDAC) is found on the outer mitochondrial membrane and allows for metabolites to enter and leave the mitochondria (Figure 10).[2] VDAC allows for ADP and P_i to enter the intermembrane space, and allows for ATP to leave the intermembrane space into the cytosol to be used as energy. To enter the matrix, ADP must go through the adenine nucleotide translocator (ANT), P_i must go through the phosphate transporter (PT), and produced ATP must leave the matrix through the ANT.[2] Overall, translocation of ADP and ATP between the matrix and the intermembrane space occurs at a 1:1 ratio, while reducing the gradient by one proton.[29] The formation of one ATP from ADP and P_i uses four protons.

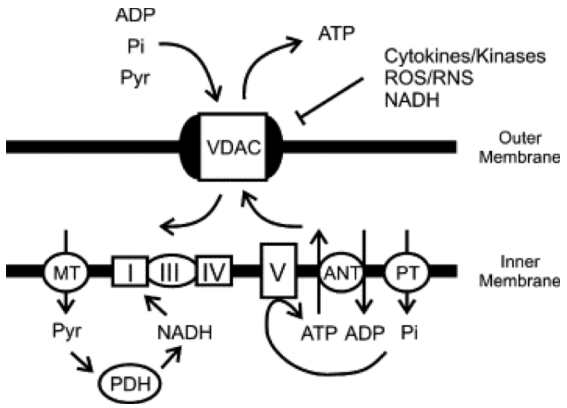

Figure 10. Representation of oxidative phosphorylation, ATP synthesis, and transporters. This figure shows complexes I-V, as well as the transporters voltage-dependent anion channel (VDAC), adenine nucleotide translocator (ANT), monocarboxylate transporter (MT), and phosphate transporter (PT). Figure reproduced with permission.[2]

OXPHOS and the Citric Acid Cycle

In addition to functioning in OXPHOS, succinate dehydrogenase (complex II) also functions in the citric acid cycle. Since reductions in complex II were observed, it is possible that the citric acid cycle is also affected by SOD2 expression. Aconitase is an enzyme that converts citrate to isocitrate (Figure 11). Aconitase is especially sensitive to ROS, since it contains a functionally important iron-sulfur center that is prone to

oxidation.[30] Following the aconitase reaction, isocitrate dehydrogenase converts isocitrate into α-ketogluterate and reduces NAD(P)$^+$ to NAD(P)H. Aconitase activity will be tested using a coupled reaction with isocitrate dehydrogenase, using the absorbance at 340 nm to measure the generation of NADPH.

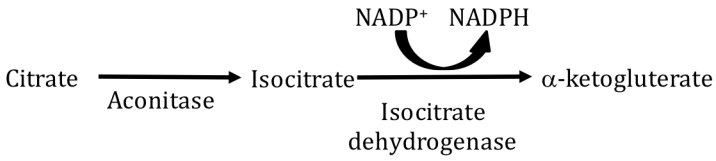

Figure 11. Reaction scheme of aconitase and isocitrate dehydrogenase. Aconitase converts citrate into isocitrate. Isocitrate dehydrogenase oxidizes isocitrate to α-ketogluterate and reduces NADP$^+$ to NADPH.

Preliminary Data

Microarrays were performed on RNA isolated from wildtype and SOD2 mouse livers to determine superoxide-dependent gene expression changes. Two wild-type and two SOD2 mice were analyzed. Although ~1,000 hepatic genes were differentially expressed in SOD2 mice compared to wild-type mice, a focus was placed on mitochondrial proteins for this project. Specifically, analysis of OXPHOS gene expression showed a decrease in nuclear encoded OXPHOS subunits and an increase

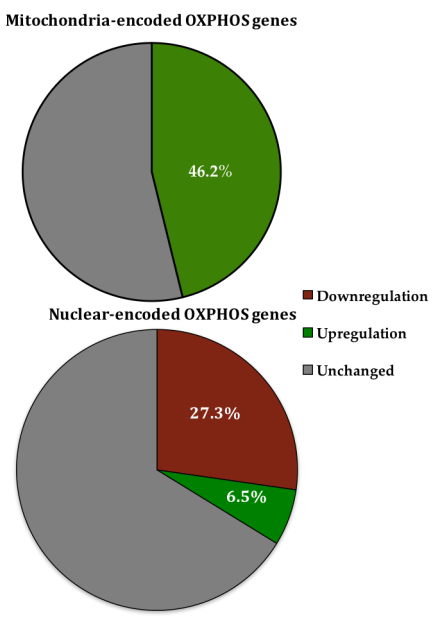

Symbol	Fold Change
MT-ND6	2.557
MT-CO3	1.356
MT-ATP6	1.242
MT-CO2	1.205
MT-ND5	1.130
MT-CYB	1.117
ATP5J	-1.219
ATP5G3	-1.232
SDHC	-1.256
NDUFS6	-1.269
NDUFS5	-1.311
NDUFAB1	-1.386
NDUFA4	-1.428
COX6B2	-1.434
NDUFB7	-1.465
UQCRC1	-1.483
SDHD	-1.497
NDUFA8	-1.514
NDUFB6	-1.705
NDUFB8	-1.734

Figure 12. Summary of preliminary microarray data. Gene expression analysis of SOD2 mice showed a decrease in 21 nuclear-encoded OXPHOS subunits and an increase in 5 of the mitochondrial encoded genes as compared to wild-type mice.

in mtDNA-encoded OXPHOS subunits. Of the nuclear-encoded OXPHOS subunits, 21 of 77 (27.3%) were downregulated in the SOD2 mice (Figure 5) and 6 of 13 mitochondria-encoded subunits (46.2%) were upregulated. This indicates a failure in mitochondria to nucleus communication, because generally an increase in mitochondria-encoded subunits correlates with an increase in nuclear-encoded subunits to retain functional complexes.

To verify microarray gene expression changes in OXPHOS complexes, sodium dodecyl sulfate polyacrylamide gel electrophoresis (SDS-PAGE) and blue native polyacrylamide gel electrophoresis (BN-PAGE) were previously performed on proteins isolated from livers of a new cohort of wild-type and SOD2 mice. Complexes II, III, and V were blotted with protein specific antibodies to observe changes in protein expression specific to each complex. 4 wild-type samples and 5 SOD2 samples were run on the SDS-PAGE. The Western blot from the SDS-PAGE gel showed a significant reduction in individual protein levels from complexes II and III, but no significant change was observed in protein levels from complex V (Figure 6A). The levels of expression in SOD2 increased in the SOD2 mutant mice compared to WT as expected. Although the expression of one protein of the complex typically indicates a reduction in assembly of the entire complex, it is important to analyze complex assembly by BN-PAGE. In BN-PAGE, detergents are selectively used to allow for migration of the intact complex through the gel. Western blots are done using antibodies against a single protein in the

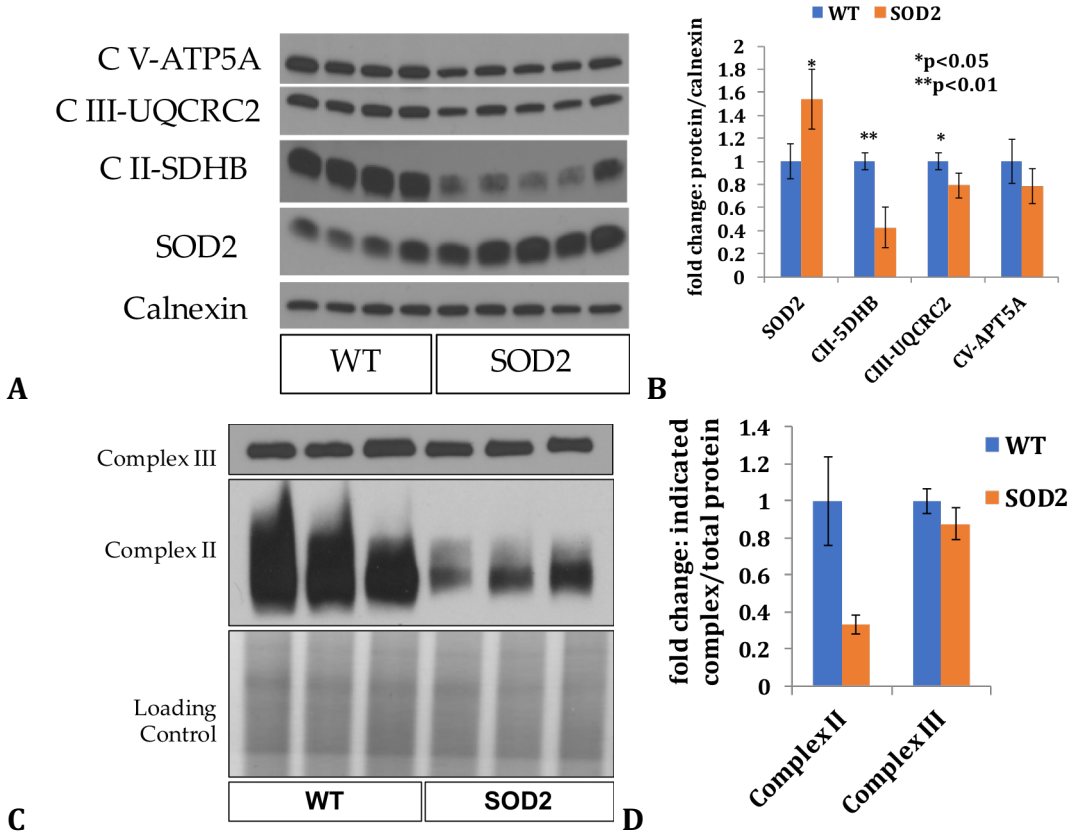

Figure 13. Previous preliminary data regarding OXPHOS gene expression. **(A)** Preliminary SDS-PAGE for complexes II, III, and V. SOD2 was blotted as a control for overexpression. **(B)** Quantitation of gene expression changes by SDS-PAGE shown in A. **(C)** Preliminary BN-PAGE for complexes II and III **(D)** Quantitation of protein bands from BN-PAGE shown in C. Figure by Yichong Zhang, reproduced with permission (personal correspondence).

complex, and the resulting band intensity is attributed to the intact complex. Preliminary BN-PAGE was run using 3 wild-type samples and 3 SOD2 samples. The Western blot showed a significant decrease in complex II in SOD2 mice similar to the SDS-PAGE results, but not in complex III (Figure 6C).

Project Goals

The focus of the current project is to verify changes in complex II by BN-PAGE in a different cohort of mice, as well as to investigate changes in other complexes. In addition, enzymatic activity of each complex will be tested. Even though OXPHOS

complexes may be reduced in expression levels, an increase in activity could potentially compensate for any expression deficits.

Methods

Antibodies

The antibodies used were NDUFS3 for complex I (1:500, Santa Cruz 374282), SDHA for complex II (1:1,000 Santa Cruz 377302), UQCRC2 for complex IV (1:500, Santa Cruz 390161) and ATP5A for complex V (1:2,500 Santa Cruz 136178). For all primary antibodies, donkey-anti-mouse secondary antibody was used (Jackson Labs).

Mice

The SOD2 transgenic mice used in this study were obtained with permission from Arlan Richardson and have been characterized extensively.[20] All work with SOD2 transgenic mice was carried out with Appalachian State IACUC and IBC approval (protocol 17-01). These mice overexpress superoxide dismutase and are maintained as heterozygotes with one copy of the transgene. Male $SOD2^{+/-}$ mice were bred with female nontransgenic (wild-type) mice. Genotyping to verify the presence of the transgene was performed by PCR analysis of DNA isolated from toe clippings of 10 day old pups. The mice were maintained in a temperature-controlled environment and fed chow. For analysis of liver proteins, male and female mice were euthanized at 10 weeks of age. A total of 8 SOD2 mice and 8 wild-type mice were used in this study. Livers from wild-type and SOD2 mice were flash frozen in liquid nitrogen and ground into a fine powder using a cold, stainless steel mortar and pestle.

Protein Quantification Assay

Protein concentration was quantified using a bicinchoninic acid (BCA) assay (#23225, Thermo Fisher Scientific). Samples were diluted 1:20 in ACBT buffer (1.5 M aminocaproic acid, 75 mM Bis-Tris, pH 7.0) prior to protein determination. In a 96-well plate, protein standards (5 µL of BSA at concentrations ranging from 0.01 to 0.05 mg/mL) were used to create a standard curve. Separately, 2 µL, 3 µL, 4 µL, and 5 µL of each sample (buffer compensated) were added to each of four different wells. A mixture of 25:24:1 parts of reagent A, reagent B, and reagent C was prepared and 200 µL was added to each well. The plate was incubated at 37 °C for 30 minutes, at which time the absorbance was measured at 562 nm. The absorbance of each sample was compared to the standard curve to determine protein concentration.

Blue-Native PAGE

Protein Isolation for Blue-Native PAGE

To isolate protein from SOD2 and wild-type mice for blue-native PAGE, ~20 mg liver powder was homogenized in a Teflon-glass Potter-Elvehjem homogenizer in 250 µL ice cold MOPS sucrose buffer (440 mM sucrose, 20 mM MOPS, 1 mM EDTA) for 6 strokes using a drill press. The homogenate was transferred to an Eppendorf tube and centrifuged at 20,000 x g for 20 minutes at 4 °C. The supernatant was removed, and 40 µL ice cold ACBT buffer was used to gently resuspend the pellet. To each sample, 3% dodecyl maltoside (DDM) was added and left on ice for 10 minutes. Samples were centrifuged at 20,000 x g for 20 minutes at 4 °C, and the pellet was discarded.

Blue-Native PAGE

BN-PAGE was performed using a precast 4%-15% Mini-Protean gel (Bio-RAD). For each lane, based on quantification of the protein from the BCA assay, 25 µg of protein were loaded along with 1X final loading dye (750 mM aminocaproic acid, 50 mM Bis-Tris, 0.5 mM EDTA, 5% Coomassie blue, pH 7.0). A high molecular weight ladder was loaded (GE 17044501). The inner chamber was filled with cathode buffer A (15 mM Bis-Tris, 50 mM Tricine, Coomassie blue 0.02%, pH 7.0) and the outer chamber was filled with clear anode buffer (50 mM Bis-tris, pH 7.0).[31] The gel was run at 30 V for 30 minutes, and then increased to 80 V. As the sample ran farther into the gradient, the current dropped below zero, and the voltage was raised to 100 V and then 110 V. After two hours (or when the blue dye front migrated halfway through the gel), the blue cathode buffer A was changed to clear cathode buffer B and run for two additional hours, until the blue dye had run out of the gel. The gel was disassembled and allowed to soak in transfer buffer (25 mM Tris, 192 mM glycine, 0.05% SDS) for 10-15 minutes prior to transfer.

The gel was then transferred to a PVDF membrane. Before the transfer, the PVDF membrane was activated in methanol for one minute. Following activation, the membrane was washed twice in water and equilibrated in ice cold transfer buffer. Proteins were transferred overnight at 30 V in the refrigerator. Prior to western blotting, the membrane was washed in water and re-equilibrated in methanol. The membrane was dried and blotted.

Western Blot

To blot for proteins within the different complexes, the dried membrane was rehydrated in 1X PBS (phosphate buffered saline, Sigma Aldrich). The membrane was

incubated overnight in the refrigerator with the respective antibody prepared in blocking buffer (PBS containing 1% casein, 0.04% Tween-20). The following day, the membrane was washed in 1X PBS for 5 minutes three times. The blot was incubated with the appropriate secondary antibody (donkey anti-mouse for all), at room temperature for one hour. Following incubation, the membrane was washed three times for 5 minutes in 1X PBS. The membrane was developed by adding the ECL substrate horseradish peroxidase (HRP, Luminata crescendo, Millipore Sigma), and the image was captured in the ChemiDoc-It Imager. A white light image was captured to visualize the ladder.

Image J Software

Changes in amount of protein between wild-type and SOD2 were quantified using Image J. Band intensities were normalized to quantification of the entire lane using the white light image of the Coomassie blue stained lane. Normalization was performed by dividing the pixels obtained for each complex by the pixels obtained from the entire lane. Each wild-type band was divided by the average of all wild-type bands to normalize wild-type to 1.0. SOD2 intensity was also normalized to the intensity of the wild-type samples.

OXPHOS Activity Assays

Mitochondrial Isolation

To isolate mitochondria, differential centrifugation was performed as described.[32] To summarize, mouse liver tissue (50 mg) was homogenized in a Teflon-glass Potter-Elvehjem homogenizer and solubilized in 0.5 mL IB_c buffer [10 mM Tris-MOPS (from 0.1 M Tris buffered to pH 7.4 with MOPS powder), 10 mM EDTA-Tris (from 0.1 M EDTA buffered to pH 7.4 with Tris powder), 0.2 M sucrose buffer, pH 7.4]. The homogenate was then transferred to an Eppendorf tube and centrifuged at 600 x g for 10 min at 4 °C. The

supernatant was transferred to a new Eppendorf tube and centrifuged at 7,000 x g for 10 min at 4 °C. The pellet from this spin was washed in IB_c buffer, and re-pelleted at 7,000 x g for 10 min at 4 °C. The pellet was then resuspended in a small amount (100 µL) of IB_c buffer and put on ice to be used fresh. The amount of protein was measured using the BCA assay kit.

NADH Dehydrogenase (Complex I) Assay

In order to determine the activity of complex I in the isolated mitochondria, methods were used as described.[33] This assay is spectrophotometric and the change in absorbance was measured at 600 nm for 5 minutes, as DCIP reduction is coupled with NADH oxidation (Figure 7). To each well, 15 µg of mitochondria (5 µL) were added as well as 195 µL of master mix. The master mix contained 2 mM KCN (to inhibit complex IV), 4 µM Antimycin A (to inhibit complex III), 100 µM decylubiquinone as the terminal electron acceptor, 3.5 mg/mL BSA, 60 µM DCIP, 150 µM NADH as the electron donor, and 80 mM Tris pH 7.4 – 0.5% Tween-80. To determine specificity of this assay for complex I, rotenone was used as an inhibitor. Rotenone inhibits the transfer of electrons from complex I to ubiquinone. Activity in the absence of rotenone was subtracted from the activity in the presence of rotenone to show activity due to complex I only. The equation used to calculate the specific activity for each of the assays was:

$$\text{Units}\times\text{mg}^{-1} = \frac{\frac{A_{600}}{\text{min}}\times 1{,}000\mu\text{M/mM} \times \text{assay volume (L)}}{\varepsilon\text{DCIP}\times\text{sample volume (mL)}\times\text{concentration}\left(\frac{\text{mg}}{\text{mL}}\right)} \qquad \text{(equation 2)}$$

Succinate Dehydrogenase (Complex II) Assay

In order to determine the activity of complex II in the mitochondria, methods from "Biochemical Assays for Mitochondrial Activity: Assays of TCA Cycle Enzymes and PDHc"

were used.[34] To summarize, 15 µg of mitochondria were incubated in 500 µL of 0.1 M Tris-HCl pH 7.4 and 100 µL of 0.2 M sodium succinate for 20 minutes at room temperature. Following preincubation, 10 µL of 0.2 M KCN, 10 µL of 5 mM DCIP, and 25 µL of 65 mM phenazine methosulfate were added. The reduction of DCIP and PMS was coupled with the oxidation of succinate to fumarate. The change in absorbance was measured at 600 nm. No inhibitor was used. Two SOD2 and two wild-type samples were used for this assay. Equation 2 was used to calculate the specific activity for each assay.

Aconitase Activity Assay

To perform an aconitase activity assay, an aconitase activity assay kit was used (#705502 Cayman Chemical). To summarize, 50 µg (50 µL) mitochondria was added to each well, along with 5 µL assay buffer, 50 µL $NADP^+$, and 50 µL isocitric dehydrogenase provided in the kit. Concentrations and components of buffers are proprietary. The reaction was initiated with 50 µL substrate solution provided. Absorbance was measured every minute for 30 minutes at 340 nm. Each sample background was measured and subtracted from the activity from the wild-type and SOD2 samples. Aconitase activity (nmol/min/mL) was determined with the following equation:

$$\frac{A_{340}(\text{sample}) - A_{340}(\text{background})}{0.00313\ \mu M^{-1}} \times \frac{\text{total volume}}{\text{protein volume}} \times \text{sample dilution} \qquad \text{(equation 3)}$$

Results and Discussion

Blue Native-PAGE

Complex I

Western blotting of NDUFS3 separated by BN-PAGE indicated no change in complex I, a subunit of complex I (Figure 14A). Quantitation of complex I band intensity normalized to the Coomassie blue stained total lane also indicated no change in complex I between wild-type and SOD2 samples (Figure 14B). A student's unpaired t-test was performed and showed no significant difference.

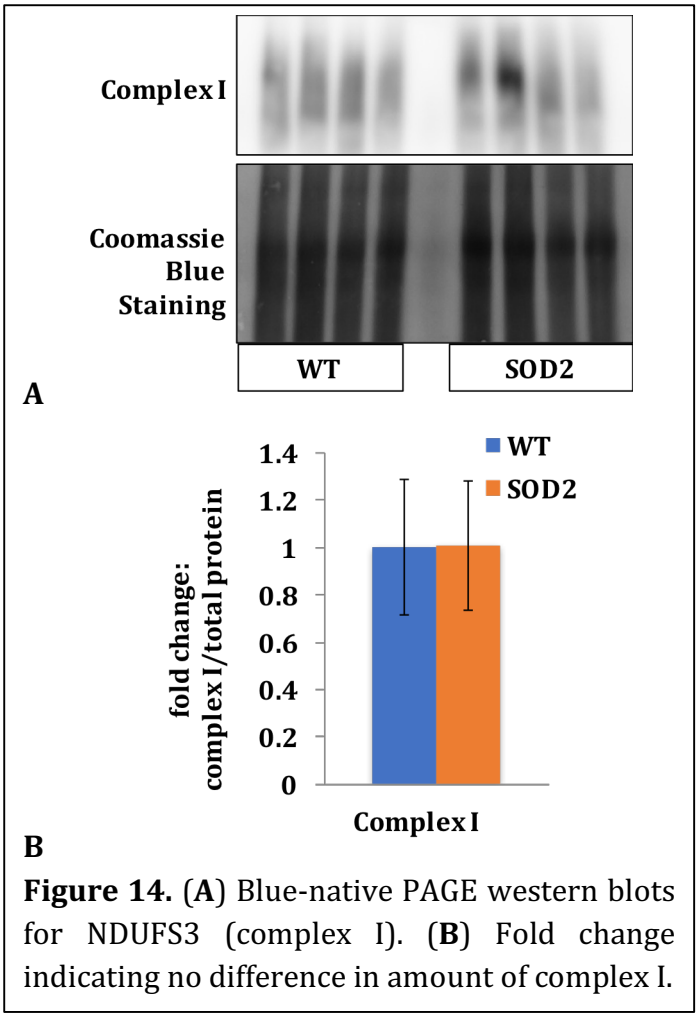

Figure 14. (**A**) Blue-native PAGE western blots for NDUFS3 (complex I). (**B**) Fold change indicating no difference in amount of complex I.

Complex II

Western blotting of complex II separated by BN-PAGE indicated a decrease in the SOD2 mice in SDHA, a subunit of complex II (Figure 15A). Quantitation of complex II band intensity normalized to the Coomassie blue stained total lane indicated a ~60% decrease in complex II in the SOD2 samples compared to the wild-type samples (Figure 15B). The complex II (wild-type and SOD2) bands were normalized to the Coomassie blue staining

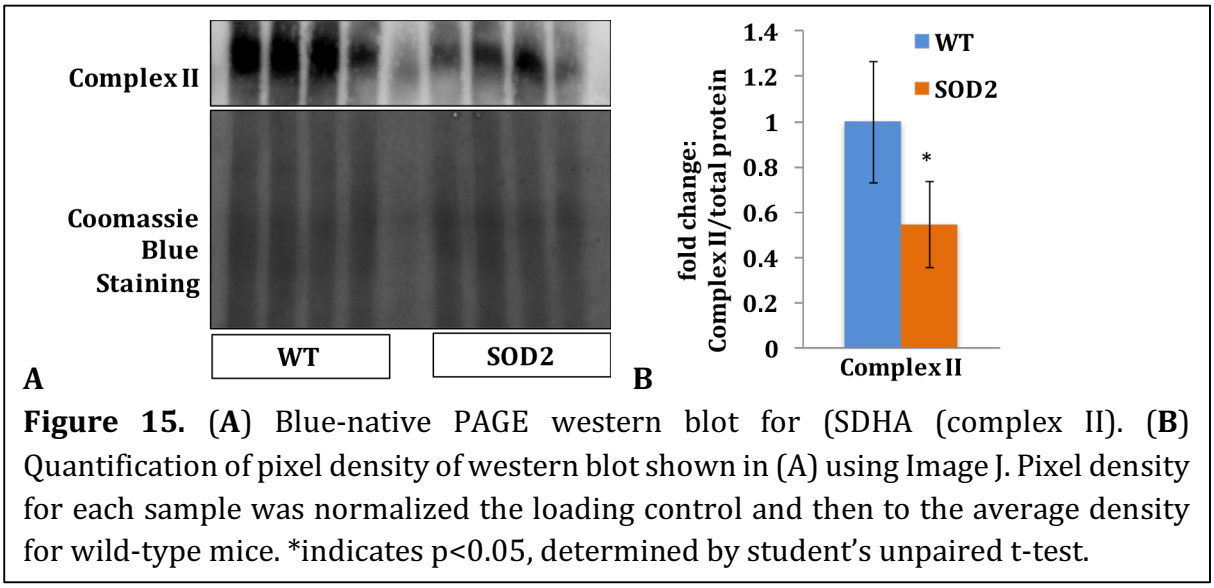

Figure 15. (**A**) Blue-native PAGE western blot for (SDHA (complex II). (**B**) Quantification of pixel density of western blot shown in (A) using Image J. Pixel density for each sample was normalized the loading control and then to the average density for wild-type mice. *indicates $p<0.05$, determined by student's unpaired t-test.

and wild-type bands and quantified (Figure 15B). This agrees with previous preliminary data obtained by Yichong Zhang based on the protein levels if SDHB (Figure 13). Repeat of this experiment in a second cohort of mice showed a similar trend but Coomassie staining was too dark and unable to be quantitated (Figure 16B).A student's t-test was performed and determined that $p<0.05$, so the values were statistically different between the SOD2 and wild-type samples for both experiments.

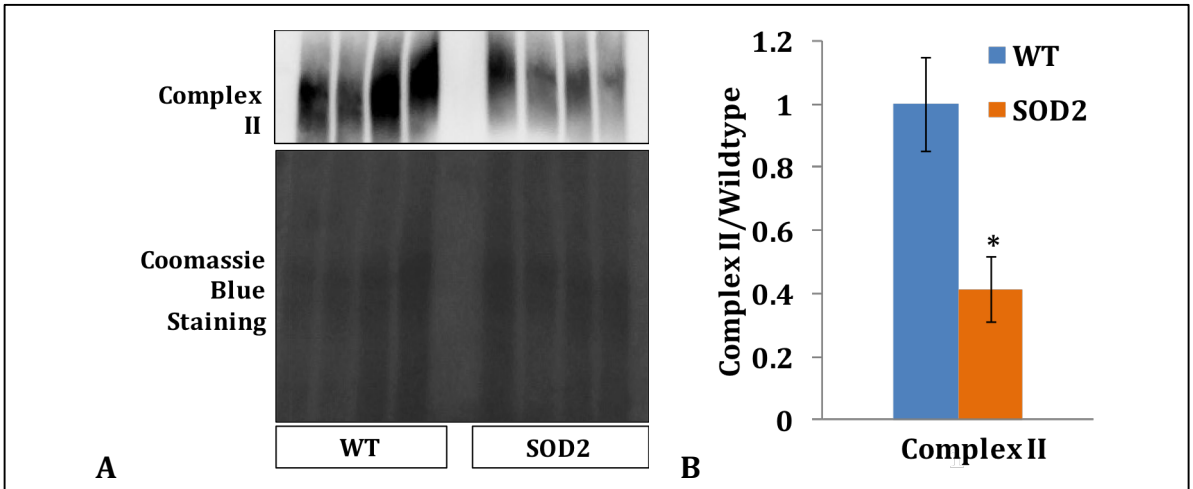

Figure 16. (**A**) Repeat of blue-native PAGE. Coomassie Blue staining from the gel could not be quantitated. (**B**) Quantification of pixel density of western blot shown in (A) using Image J. Pixel density for each sample was normalized to the average density for wild-type mice. *indicates $p<0.05$, determined by student's unpaired t-test.

Complex III

Western blotting of complex III separated by BN PAGE indicated no change in UQCRC2, a subunit of complex III (Figure 17A). Quantitation of complex III band intensity normalized to the Coomassie blue stained total lane confirmed no change in complex III between wild-type and SOD2 samples (Figure 17B). A student's unpaired t-test was performed to determine that $p>0.05$, and SOD2 samples were not statistically different from wild-type samples. This agrees with the preliminary data in experiments performed by Yichong Zhang showing no difference in UQCRC2 for complex III (Figure 13).

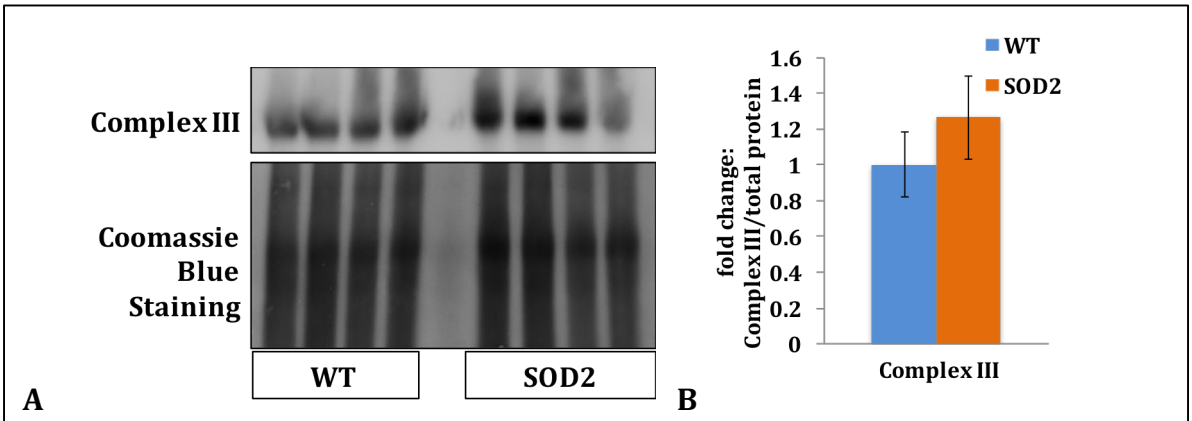

Figure 17. (**A**) Blue-native PAGE western blots for Complex III. (**B**) Fold change for complex II determined by quantitating pixel density using Image J.

Complex V

Western blotting of complex V separated by BN PAGE indicated a decrease in ATP5A, a subunit of complex V (Figure 18A). Quantitation of complex V band intensity normalized to the Coomassie blue stained total protein lane indicated a ~60% decrease in ATP5A levels in the SOD2 samples compared to the wild-type samples (Figure 18B). The BN-PAGE was repeated in a different cohort of mice, the first being from liver samples brought from Yale, and the repeat from tissue harvested from mice at Appalachian State University. The results from the second cohort of mice agree that there is a decrease in complex V in the SOD2 samples compared to the wild-type samples (Figure 19).

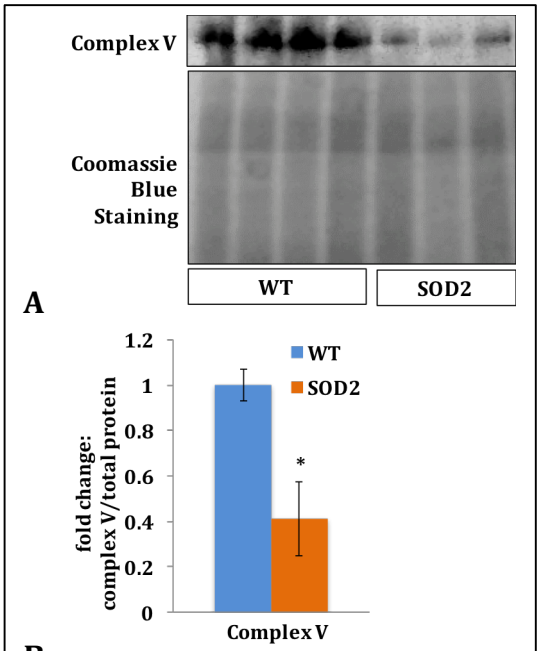

Figure 18. (**A**) Blue-native PAGE western blots for Complex V. (**B**) Fold change for complex V determined by quantitating pixel density using Image J. * indicates $p<0.05$, determined by student's unpaired t-test.

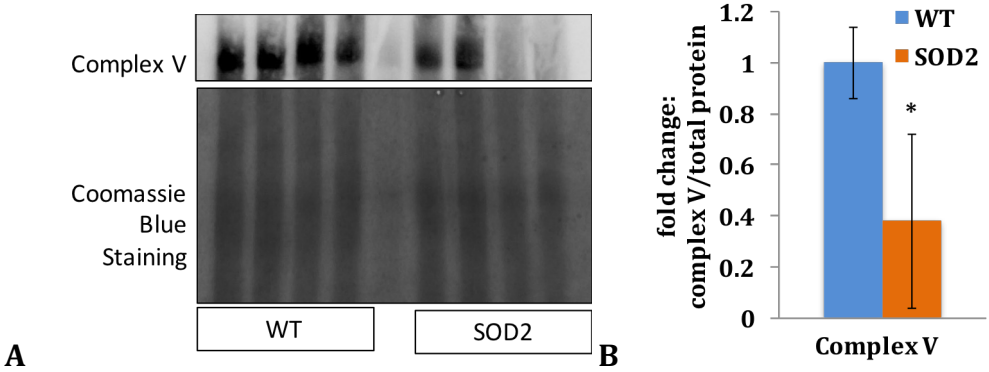

Figure 19. (**A**) Repeated Blue-native PAGE western blots for Complex V. (**B**) Fold change for complex II determined by quantitating pixel density using Image J. * indicates $p<0.05$, determined by student's unpaired t-test.

Activity Assays

NADH Dehydrogenase Activity Assay

An NADH dehydrogenase (complex I) activity assay was run by incubating mitochondria with NADH as the electron donor and decylubiquinone as the electron acceptor. The DCIP-coupled NADH dehydrogenase is characterized by a reduction in the absorbance at 600 nm. DCIP in its reduced form has no absorbance at this wavelength, therefore as the assay proceeds, there is a colorimetric change from blue to clear. Rotenone, which inhibits complex I, was used to determine complex I specificity of the color change. Although the presence of rotenone should show a 70-80% reduction in slope, no change was observed. Assays with serial dilutions of rotenone were run to try and find the optimal concentration of rotenone necessary to inhibit complex I (Figure 20). Concentrations of 0.125 μM to 4 μM rotenone were used in the activity assay, but none of these inhibited complex I.

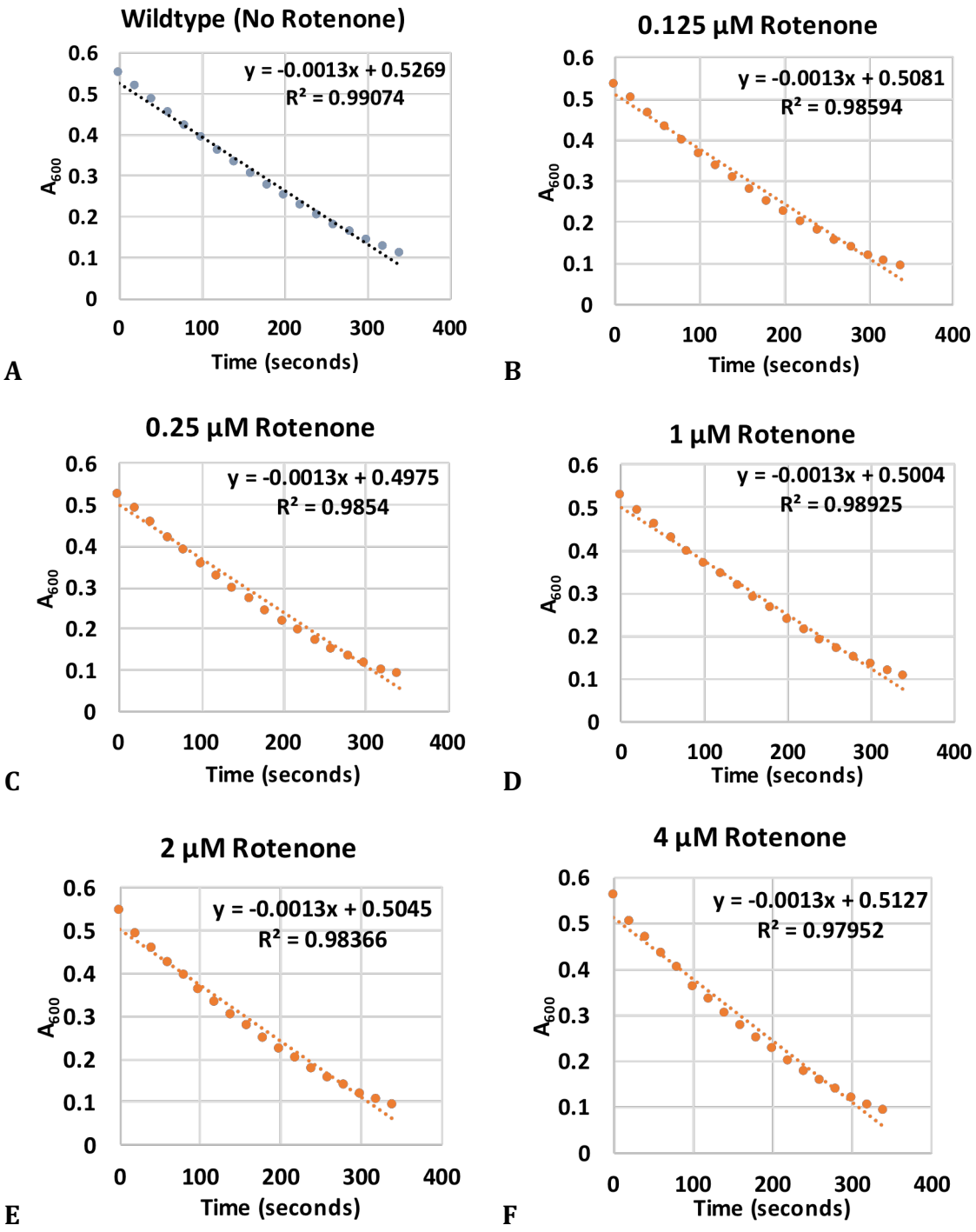

Figure 20. Complex I activity assays. (**A**) shows no rotenone and (**B-F**) show serial dilutions of rotenone from 0.125 µM rotenone to 4 µM rotenone. Rotenone did not inhibit NADH oxidation at any concentration.

To troubleshoot further, each component of the assay was sequentially removed in a series of control reactions. Conditions tested were: no mitochondria, no NADH, no cyanide, no antimycin A, no BSA, and no decylubiquinone (Figure 21). In the absence of mitochondria, no activity was observed (Figure 21A, B, F). Similarly, in the absence of NADH, no activity was observed (Figure 21B). None of the trials adding rotenone resulted in a change in slope (Figure 21A, C, D, E). Importantly, the assay in the absence of decylubiquinone still showed activity, indicating that the assay is decylubiquinone independent. There was a 15% difference when the mitochondria were treated with rotenone for five minutes before starting the reaction with the master mix and NADH (Figure 22). The average rotenone-sensitive specific activity at 600 nm for the wild-type samples was 0.00604 U/mg, and the average rotenone-sensitive specific activity at 600 nm for SOD2 samples was 0.0121 U/mg (Figure 22E).

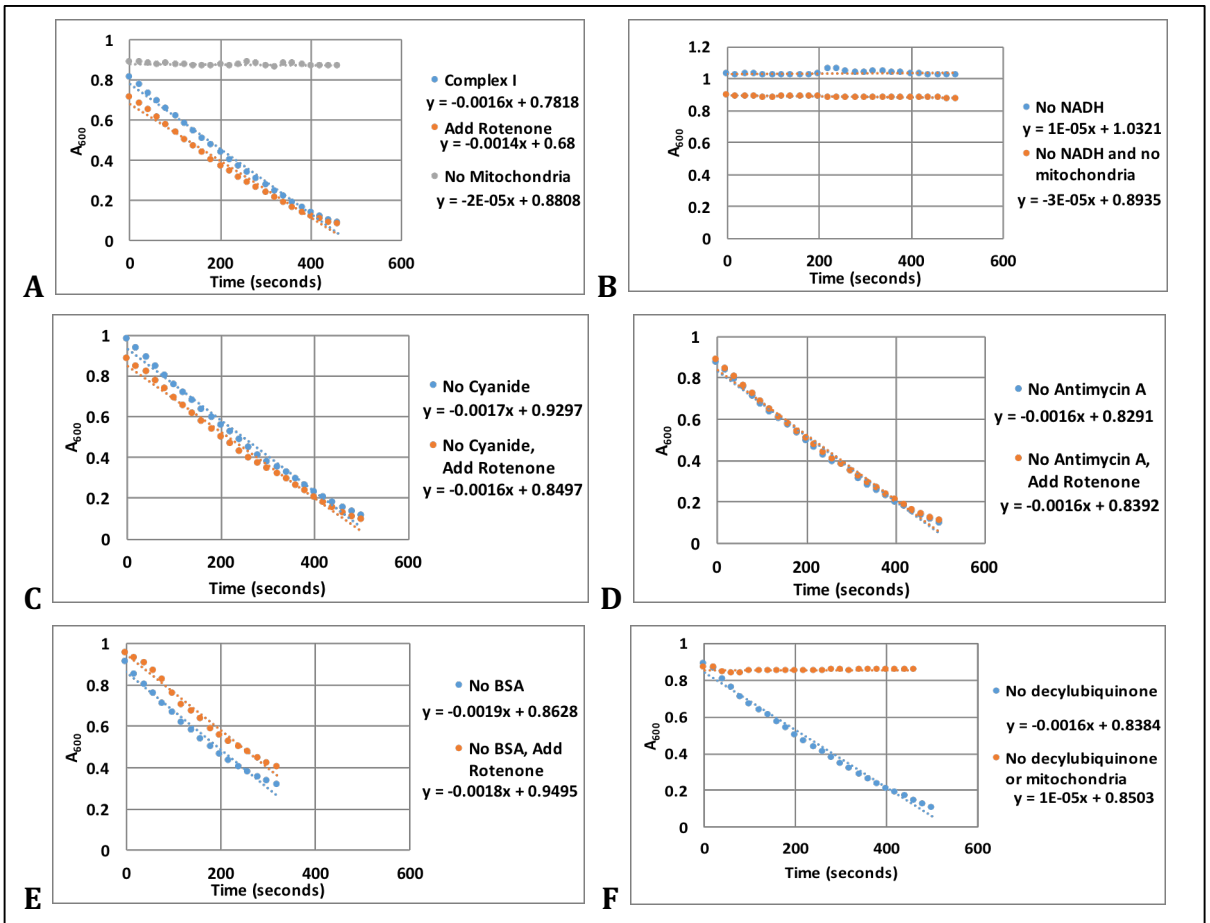

Figure 21. Complex I activity assays. (A) compares activity with or without rotenone, and shows a control with no mitochondria. (B) shows controls with either no NADH or with no NADH nor mitochondria. (C) shows controls with no cyanide, both with or without rotenone. (D) shows controls with no antimycin A, both with or without rotenone. (E) shows controls with no BSA, both with or without rotenone. (F) shows controls with no decylubiquinone or with no decylubiquinone nor mitochondria.

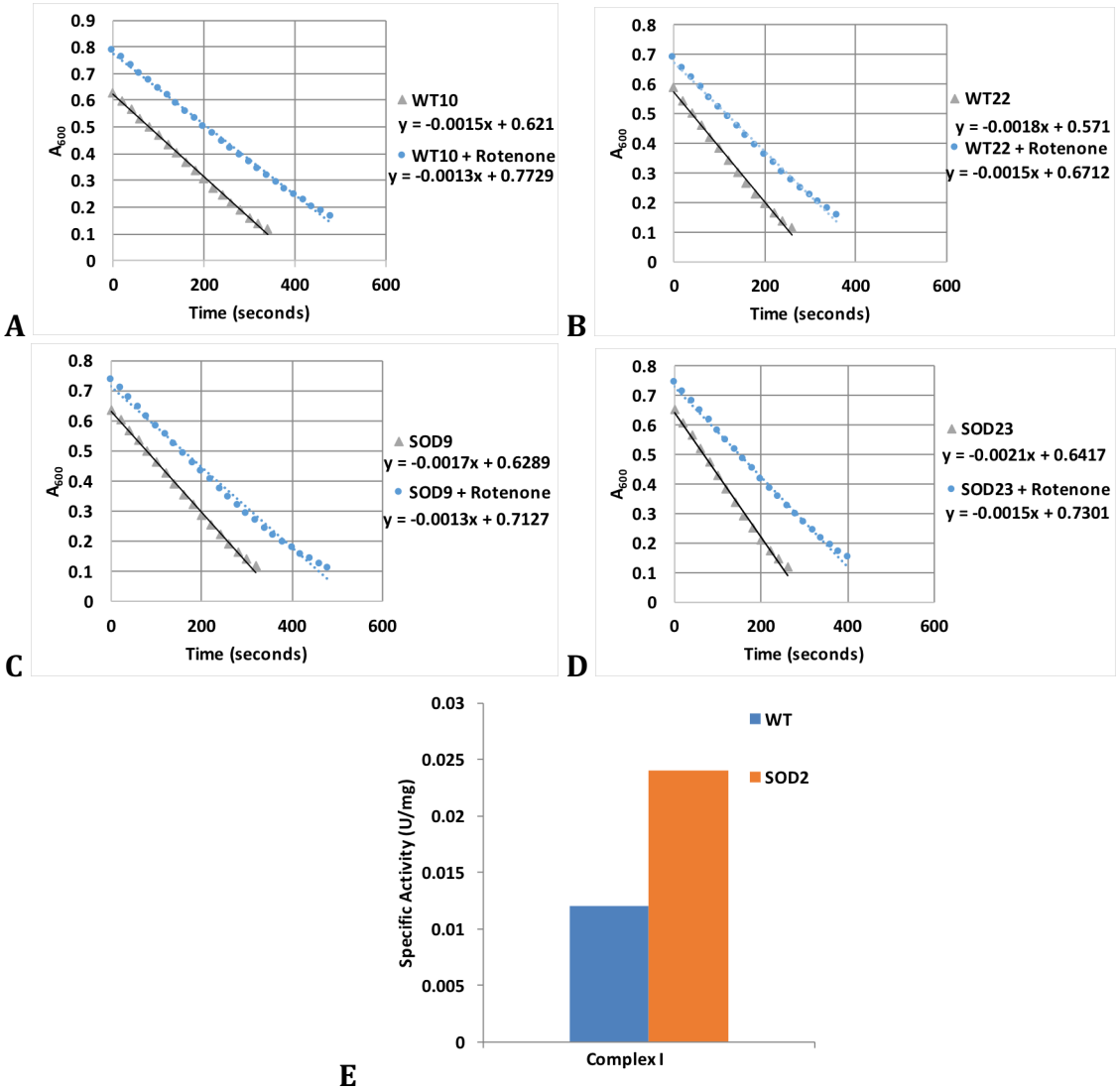

Figure 22. Complex I activity assays **(A and B)** Change in absorbance of DCIP measured at 600 nm coupled with NADH oxidation for wild-type samples. **(C and D)** Change in absorbance of DCIP measured at 600 nm coupled with NADH oxidation for SOD2 samples. **(E)** Average rotenone-sensitive specific activity for both wild-type and SOD2 samples. There are no error bars, as data was collected from only two samples.

Succinate Dehydrogenase Activity Assay

Activity of succinate dehydrogenase was tested by incubating mitochondria from wild-type samples and SOD2 samples with succinate as the electron donor and decylubiquinone as the electron acceptor. The assay shows a slight reduction in the activity of complex II in the SOD2 samples compared to the wild-type samples (Figure 23). This change in activity does not represent the 60% decrease in the amount of complex II observed in the Western blot for SOD2 samples. Figures 23A and 23B were not normalized to the amount of mitochondria in each sample. Figure 23C shows the activity (U/mg) normalized to the amount of mitochondria in each sample determined using equation 2.

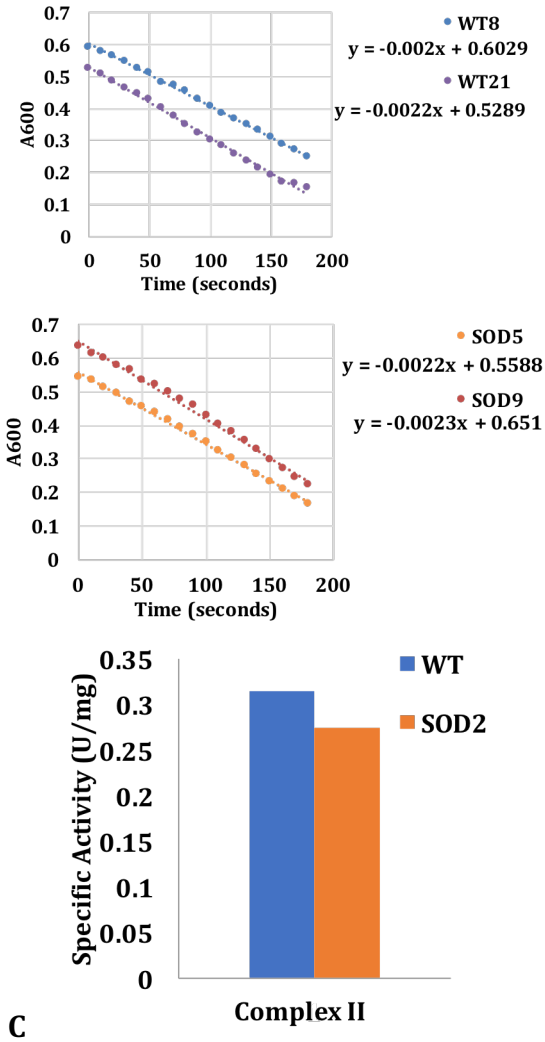

Figure 23. Complex II activity assays. (**A**) Decrease in absorbance due to the activity of complex II in wild-type samples. (**B**) Decrease in absorbance due to the activity of complex II in SOD2 samples. (**C**) Fold change normalized to amount of protein input into the assay. In Figures A and B, the same volume was loaded into each sample, but not the same amount of mitochondria. Once the protein amount was determined for each sample, the activity was normalized in figure C. There are no error bars, as the data is from two samples.

Aconitase Activity Assay

Because complex II functions in both the citric acid cycle and OXPHOS, aconitase activity was measured to show whether there was citric acid cycle dysfunction. An aconitase activity assay kit was used to determine the amount of aconitase activity in the citric acid cycle. The aconitase assay shows an increase in activity for the SOD2 samples compared to the wild-type samples (Figure 24). This agrees with a previous study showing a slight increase in aconitase activity in skeletal muscle in young mice.[20]

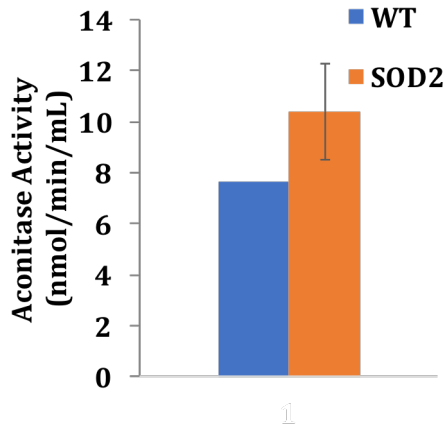

Figure 24. Aconitase activity in two wild-type and three SOD2 samples. Error bars are missing on the wild-type samples because only two samples were able to be quantified from the A_{600}.

Discussion

Complex I Abundance and Activity

Preliminary studies were unable to ascertain differences in abundance of complex I by SDS-PAGE. The antibodies available for Complex I are extraordinarily sensitive to heat. Therefore, it was determined that BN-PAGE was a better experiment to determine complex I abundance. No change was observed in the amount of intact complex I by BN-PAGE between wild-type and SOD2 mice. Preliminary activity assays in the current study indicated SOD2 mice had slightly increased activity of complex I. However, a problem with the interpretation of the activity assay is that the rotenone-sensitive activity was less than has been reported (70-80%).[35] The initial conclusion of increased activity is

based on a 15% rotenone-sensitive activity. Despite testing serial dilutions of rotenone, no concentration was able to effectively inhibit complex I. Rotenone sensitivity has been reported to be less in the liver than in other tissues[7], presumably due to the high level of NADH-dependent enzymes in liver mitochondria (malate dehydrogenase, pyruvate dehydrogenase, alpha-ketogluterate dehydrogenase, etc.). These additional enzymes are rotenone insensitive and would therefore increase observed background activity.

A number of control reactions were run that tested each component of the assay. The first few trials tested activity in the presence and absence of rotenone, but no rotenone-sensitivity was observed (Figure 22A). As expected, mitochondria were required to convert NADH to NAD^+. Since NADH is the substrate of the reaction, it was also not surprising that the reaction failed to proceed in the absence of NADH (Figure 22B). It was problematic that the reaction proceeded in the absence of cyanide or antimycin A. Cyanide is an inhibitor of complex IV, and antimycin A is an inhibitor of complex III. It is important to inhibit these complexes, as they are downstream of complexes I and II and any deficiency in downstream complexes could be falsely interpreted as a deficiency in complex I. Complexes III and IV would also accept electrons in place of the terminal electron acceptor, and thus would interfere in the assay readout. BSA is used in the assay to increase the solubility of decylubiquinone and rotenone[36], but had no effect when removed from the assay (Figure 22E). The most striking observation in the control reactions was that the absorbance in the assay proceeded to decrease at 600 nm in the absence of decylubiquinone, the terminal electron acceptor (Figure 22F). The activity assay depends on the transfer of electrons from complex I to decylubiquinone, and then from decylubiquinone to DCIP. In the absence of

decylubiquinone, it is not clear how electrons would be transferred to DCIP directly. It is possible that DCIP is accepting electrons directly from NADH, which would indicate that the observed activity is not due to complex I, as complex DCIP does not react efficiently with complex I.[37] There may also be a sufficient pool of ubiquinone in the mitochondria samples such that additional decylubiquinone is not necessary. To eliminate secondary electron transfer effects an alternative for this activity assay would be to measure the absorbance at 340 nm, since NADH absorbs at that wavelength and NAD^+ does not. However, mitochondria tend to have a high background absorbance at 340 nm, which interferes in this assay.

Complex II Abundance and Activity

The preliminary microarray showed that three of the four proteins that make up complex II are downregulated, with the fourth being unchanged. BN-PAGE for complex II shows a decrease in the amount of total complex assembly in the SOD2 mice compared to the wild-type mice (Figures 15 and 16). This reduction agrees with preliminary data that showed a decrease in complex II by both BN-PAGE and SDS-PAGE (Figure 13). The complex II activity assay showed that SOD2 mice display slightly reduced activity of succinate dehydrogenase; however, more samples need to be analyzed to confirm significance since standard deviation cannot be determined. Additionally, given the issues with inhibitor-sensitivity of complex I, this assay should be repeated in the presence of malonate, an inhibitor of complex II. Since no other mitochondrial enzymes use succinate as a substrate, malonate inhibition is typically not performed.

When the activity from complexes I and II are analyzed, it appears that SOD2 mice have increased complex I activity and decreased complex II activity. Since both of these

complexes contribute to the decylubiquinol pool, they are in a way functionally redundant. It is possible that because complex II is reduced in abundance and activity, complex I is increasing activity as a compensatory mechanism.

Complex III Abundance

Preliminary studies indicated no change in complex III, and a confirmation BN-PAGE using additional wild-type ad SOD2 mice confirmed this finding. Since BN-PAGE and SDS-PAGE indicated no change in complex abundance, no activity assays were performed for this complex.

Complex V Abundance

Preliminary SDS-PAGE indicated no change in complex V. However, BN-PAGE in current studies shows a decrease in assembly of this complex in SOD2 samples. Current studies have repeated this experiment using two cohorts of mice, which both indicated reduced complex V assembly in SOD2 mice (Figures 18 and 19). It is critical that ATP production in these samples be measured in order to confirm a functional consequence of reduced complex assembly.

Complex II and the Citric Acid Cycle

One of the most striking observations in this study is the reduction in complex II since complex II functions in the citric acid cycle as well as OXPHOS. Analysis of citric acid cycle activity by the aconitase activity assay showed an increase in the SOD2 samples. This agrees with previous studies that also showed an increase in aconitase activity in SOD2 mice in muscle.[20] It is unusual to have high levels of aconitase upstream of a dysfunctional succinate dehydrogenase, since a buildup of succinate could cause product inhibition of aconitase. However, since the citric acid cycle is the metabolic hub of the

cell, intermediates of the cycle could be leaving to affect other pathways. For example, succinyl-CoA can leave the citric acid cycle and combine with glycine in the first step of porphyrin synthesis.[38]

Aconitase is ROS sensitive because ROS have the ability to damage its iron sulfur centers.[30] Superoxide oxidizes the iron and is reduced to hydrogen peroxide. In the presence of increased SOD2, reduced oxidative damage to aconitase is thought to cause its increased activity. The aconitase assay indicates no defect in the early phases of citric acid cycle upstream of succinate dehydrogenase. This assay also looks at overall citric acid cycle health. However, downstream enzymes (fumarase and malate dehydrogenase) and pathways such as porphyrin synthesis still need to be tested.

Conclusion/Future Plans

Currently there is not an assay to use that looks at the amount of ROS in tissue, which would be beneficial to determine the amount of superoxide and hydrogen peroxide found in the mitochondria. Knowing this would show whether SOD2 mice have increased levels of hydrogen peroxide compared to wild-type mice. If SOD2 mice have more hydrogen peroxide than wild-type mice, this ROS could be affecting the OXPHOS complexes.

Because aconitase is increased and succinate dehydrogenase is decreased in SOD2 mice, a complete metabolic analysis of the citric acid cycle pathways is needed to determine which are upregulated and which are downregulated. This would help determine which intermediates are leaving to perform other functions, and which are inhibited due to the inhibition of succinate dehydrogenase.

References

1. Taanman, J. W., The mitochondrial genome: structure, transcription, translation and replication. *Biochim Biophys Acta* **1999,** *1410* (2), 103-23.
2. Lemasters, J. J.; Holmuhamedov, E., Voltage-dependent anion channel (VDAC) as mitochondrial governator--thinking outside the box. *Biochim Biophys Acta* **2006,** *1762* (2), 181-90.
3. Liou, G. Y.; Storz, P., Reactive oxygen species in cancer. *Free Radic Res* **2010,** *44* (5), 479-96.
4. Barja, G., Free radicals and aging. *Trends Neurosci* **2004,** *27* (10), 595-600.
5. Paglialunga, S.; Ludzki, A.; Root-McCaig, J.; Holloway, G. P., In adipose tissue, increased mitochondrial emission of reactive oxygen species is important for short-term high-fat diet-induced insulin resistance in mice. *Diabetologia* **2015,** *58* (5), 1071-80.
6. Hureau, C.; Faller, P., Abeta-mediated ROS production by Cu ions: structural insights, mechanisms and relevance to Alzheimer's disease. *Biochimie* **2009,** *91* (10), 1212-7.
7. Spinazzi, M.; Casarin, A.; Pertegato, V.; Salviati, L.; Angelini, C., Assessment of mitochondrial respiratory chain enzymatic activities on tissues and cultured cells. *Nat Protoc* **2012,** *7* (6), 1235-46.
8. Gautheron, D. C., Mitochondrial oxidative phosphorylation and respiratory chain: review. *J Inherit Metab Dis* **1984,** *7 Suppl 1*, 57-61.
9. Duan, M.; Tu, J.; Lu, Z., Recent Advances in Detecting Mitochondrial DNA Heteroplasmic Variations. *Molecules* **2018,** *23* (2).
10. Yin, P. H.; Lee, H. C.; Chau, G. Y.; Wu, Y. T.; Li, S. H.; Lui, W. Y.; Wei, Y. H.; Liu, T. Y.; Chi, C. W., Alteration of the copy number and deletion of mitochondrial DNA in human hepatocellular carcinoma. *Br J Cancer* **2004,** *90* (12), 2390-6.
11. Anderson, S.; Bankier, A. T.; Barrell, B. G.; de Bruijn, M. H.; Coulson, A. R.; Drouin, J.; Eperon, I. C.; Nierlich, D. P.; Roe, B. A.; Sanger, F.; Schreier, P. H.; Smith, A. J.; Staden, R.; Young, I. G., Sequence and organization of the human mitochondrial genome. *Nature* **1981,** *290* (5806), 457-65.
12. Turrens, J. F., Mitochondrial formation of reactive oxygen species. *J Physiol* **2003,** *552* (Pt 2), 335-44.
13. Ray, P. D.; Huang, B. W.; Tsuji, Y., Reactive oxygen species (ROS) homeostasis and redox regulation in cellular signaling. *Cell Signal* **2012,** *24* (5), 981-90.
14. Ambrosone, C. B.; Freudenheim, J. L.; Thompson, P. A.; Bowman, E.; Vena, J. E.; Marshall, J. R.; Graham, S.; Laughlin, R.; Nemoto, T.; Shields, P. G., Manganese superoxide dismutase (MnSOD) genetic polymorphisms, dietary antioxidants, and risk of breast cancer. *Cancer Res* **1999,** *59* (3), 602-6.
15. Finkel, T.; Holbrook, N. J., Oxidants, oxidative stress and the biology of ageing. *Nature* **2000,** *408* (6809), 239-47.
16. Ames, B. N.; Gold, L. S.; Willett, W. C., The causes and prevention of cancer. *Proc Natl Acad Sci U S A* **1995,** *92* (12), 5258-65.
17. Schieber, M.; Chandel, N. S., ROS function in redox signaling and oxidative stress. *Curr Biol* **2014,** *24* (10), R453-62.

18. Fukai, T.; Ushio-Fukai, M., Superoxide dismutases: role in redox signaling, vascular function, and diseases. *Antioxid Redox Signal* **2011,** *15* (6), 1583-606.
19. Zelko, I. N.; Mariani, T. J.; Folz, R. J., Superoxide dismutase multigene family: a comparison of the CuZn-SOD (SOD1), Mn-SOD (SOD2), and EC-SOD (SOD3) gene structures, evolution, and expression. *Free Radic Biol Med* **2002,** *33* (3), 337-49.
20. Jang, Y. C.; Perez, V. I.; Song, W.; Lustgarten, M. S.; Salmon, A. B.; Mele, J.; Qi, W.; Liu, Y.; Liang, H.; Chaudhuri, A.; Ikeno, Y.; Epstein, C. J.; Van Remmen, H.; Richardson, A., Overexpression of Mn superoxide dismutase does not increase life span in mice. *J Gerontol A Biol Sci Med Sci* **2009,** *64* (11), 1114-25.
21. Holley, A. K.; Bakthavatchalu, V.; Velez-Roman, J. M.; St Clair, D. K., Manganese superoxide dismutase: guardian of the powerhouse. *Int J Mol Sci* **2011,** *12* (10), 7114-62.
22. Lenaz, G.; Fato, R.; Genova, M. L.; Bergamini, C.; Bianchi, C.; Biondi, A., Mitochondrial Complex I: structural and functional aspects. *Biochim Biophys Acta* **2006,** *1757* (9-10), 1406-20.
23. Rutter, J.; Winge, D. R.; Schiffman, J. D., Succinate dehydrogenase - Assembly, regulation and role in human disease. *Mitochondrion* **2010,** *10* (4), 393-401.
24. Spaar, A.; Flock, D.; Helms, V., Association of cytochrome c with membrane-bound cytochrome c oxidase proceeds parallel to the membrane rather than in bulk solution. *Biophys J* **2009,** *96* (5), 1721-32.
25. Matsuno-Yagi, A.; Hatefi, Y., Ubiquinol:cytochrome c oxidoreductase (complex III). Effect of inhibitors on cytochrome b reduction in submitochondrial particles and the role of ubiquinone in complex III. *J Biol Chem* **2001,** *276* (22), 19006-11.
26. Kim, H.; Esser, L.; Hossain, M. B.; Xia, D.; Yu, C. A.; Riso, J.; van der Helm, D.; Deisenhofer, J., Structure of antimycin A1, a specific electron transfer inhibitor of ubiquinol-cytochrome c oxidoreductase. *J Am Chem Soc* **1999,** *121* (20), 4902-4903.
27. Li, Y.; Park, J. S.; Deng, J. H.; Bai, Y., Cytochrome c oxidase subunit IV is essential for assembly and respiratory function of the enzyme complex. *J Bioenerg Biomembr* **2006,** *38* (5-6), 283-91.
28. Dimroth, P.; Kaim, G.; Matthey, U., Crucial role of the membrane potential for ATP synthesis by F(1)F(o) ATP synthases. *J Exp Biol* **2000,** *203* (Pt 1), 51-9.
29. Chinopoulos, C.; Vajda, S.; Csanady, L.; Mandi, M.; Mathe, K.; Adam-Vizi, V., A novel kinetic assay of mitochondrial ATP-ADP exchange rate mediated by the ANT. *Biophys J* **2009,** *96* (6), 2490-504.
30. Beinert, H.; Kennedy, M. C.; Stout, C. D., Aconitase as Ironminus signSulfur Protein, Enzyme, and Iron-Regulatory Protein. *Chem Rev* **1996,** *96* (7), 2335-2374.
31. Fiala, G. J.; Schamel, W. W.; Blumenthal, B., Blue native polyacrylamide gel electrophoresis (BN-PAGE) for analysis of multiprotein complexes from cellular lysates. *J Vis Exp* **2011,** (48).
32. Frezza, C. C., S; Scorrano, L, Organelle isolation: functional mitochondria from mouse liver, muscle and cultured filroblasts
. *Nature* **2007,** *2*, 287-295.
33. Barrientos, A.; Fontanesi, F.; Diaz, F., Evaluation of the mitochondrial respiratory chain and oxidative phosphorylation system using polarography and spectrophotometric enzyme assays. *Curr Protoc Hum Genet* **2009,** *Chapter 19*, Unit19 3.

34. Reisch, A. S.; Elpeleg, O., Biochemical assays for mitochondrial activity: assays of TCA cycle enzymes and PDHc. *Methods Cell Biol* **2007,** *80*, 199-222.
35. Heinz, S.; Freyberger, A.; Lawrenz, B.; Schladt, L.; Schmuck, G.; Ellinger-Ziegelbauer, H., Mechanistic Investigations of the Mitochondrial Complex I Inhibitor Rotenone in the Context of Pharmacological and Safety Evaluation. *Sci Rep* **2017,** *7*, 45465.
36. Janssen, A. J.; Trijbels, F. J.; Sengers, R. C.; Smeitink, J. A.; van den Heuvel, L. P.; Wintjes, L. T.; Stoltenborg-Hogenkamp, B. J.; Rodenburg, R. J., Spectrophotometric assay for complex I of the respiratory chain in tissue samples and cultured fibroblasts. *Clin Chem* **2007,** *53* (4), 729-34.
37. Jones, A. J.; Hirst, J., A spectrophotometric coupled enzyme assay to measure the activity of succinate dehydrogenase. *Anal Biochem* **2013,** *442* (1), 19-23.
38. Chung, J.; Chen, C.; Paw, B. H., Heme metabolism and erythropoiesis. *Curr Opin Hematol* **2012,** *19* (3), 156-62.